Comparing UAV and Pole Photogrammetry for Monitoring Beach Erosion

Jack Joseph Gonzales

Thesis submitted to the faculty of the Virginia Polytechnic Institute and State University
in partial fulfillment of the requirements for the degree of

Master of Science
In
Geography

Thomas Pingel, Chair/Advisor
Tina Dura
Yang Shao

August 25th, 2021
Blacksburg, VA

Keywords: Photogrammetry, Coastal erosion, UAVs, Land change monitoring

Comparing UAV and Pole Photogrammetry for Monitoring Beach Erosion

Jack Joseph Gonzales

Abstract

Sandy beaches are vulnerable to extreme erosion during large storms, as well as gradual erosion processes over months and years. Without monitoring and adaptation strategies, erosion can put people, homes, and other infrastructure at risk. To effectively manage beach resources and respond to erosion hazards, coastal managers must have a reliable means of surveying the beach to monitor erosion and accretion. These elevation surveys typically incorporate traditional ground-based surveying methods or lidar surveys flown from large, fixed-wing aircraft. While both strategies are effective, advancements in photogrammetric technology offers a new solution for topographic surveying: Structure from Motion (SfM). Using a set of overlapping aerial photographs, the SfM workflow can generate accurate topographic surveys, and promises to provide a fast, inexpensive, and reliable method for routine beach surveying. Unmanned aerial vehicles (UAVs) are often successfully employed for SfM surveys but can be limited by poor weather ad government regulations, which can make flying difficult or impossible. To circumvent these limitations, a digital camera can be attached to a tall pole on a mobile platform to obtain aerial imagery, avoiding the restrictions of UAV flight. This thesis compares these two techniques of image acquisition for routine beach monitoring. Three surveys were conducted at monthly intervals on a beach on the central South Carolina coast, using both UAV and pole photogrammetry. While both methods use the same software and photogrammetric workflow, the UAV produced better results with far fewer processing artifacts compared to pole photogrammetry.

Comparing UAV and Pole Photogrammetry for Monitoring Beach Erosion

Jack Joseph Gonzales

General Audience Abstract

Beach environments are vulnerable to extreme erosion, especially in the face of sea level rise and large storms like hurricanes. Monitoring erosion is a crucial part of a coastal management strategy, to mitigate risk to coastal hazards like extreme erosion, storm surge, and flooding. Erosion monitoring usually involves repeated elevation surveys to determine how much sand is being lost from the beach, and where that sand is being eroded away. Within the past decade, Structure from Motion (SfM) photogrammetry, the process of deriving ground elevation maps from multiple overlapping aerial photographs, has become a common technique for repeated elevation surveys. Unmanned aerial vehicles (UAVs) are often used to gather aerial imagery for SfM elevation surveys but are limited by poor weather conditions and government flight regulations, both of which can prohibit flight. However, similar aerial photographs can be taken with a camera mounted atop a tall pole, which can be used in wider range of weather conditions and without government regulations, providing an alternative when UAV flight is not an option. This study compares these two platforms for routine beach erosion monitoring surveys, evaluating them based on performance, cost, and feasibility. The UAV system is found to be fast, affordable, and effective, while the pole photogrammetry system is heavily affected by the slow speed of surveying and processing errors that make it unusable without significant improvement.

Dedication

Ut in omnibus glorificetur Deus.

Acknowledgments

I must first thank my family for their unwavering love and support, without which I would be lost. A special thanks goes to my uncle, Manny Gonzales for accompanying me on my field excursions, which would not have been possible alone. I must also thank *Battlestag* and *Local Cluster* for diligently carrying us to and from the island.

Next, I would like to thank my advisor, Dr. Thomas Pingel for all his guidance the past two years, especially for helping me work through the weeds of photogrammetric processing and always keeping me on top of things.

I would also like to express my gratitude to Dr. Anamaria Bukvic, for offering me a research assistantship and giving me the opportunity to engage in exciting coastal research beyond my thesis topic.

I must thank all my beloved friends I have made over the past two years for all the joy and love that you bring. This degree is not the finest gem I have found in Blacksburg.

Finally, I thank the sea, the deeps, and living creatures that creep, for being such a beautiful study area, and for their challenge to look beyond and explore the depths.

Table of Contents

List of Figures

1. Introduction

Structure from Motion (SfM) photogrammetry has become a mature technology widely used in geomorphometric applications, including to model sandy beaches specifically (Eltner et al., 2016; Harwin and Lucieer, 2012; James and Robson, 2012; James and Robson, 2014; Mancini et al., 2013; Taddia et al., 2020; Turner et al., 2016; Westoby et al., 2012). SfM surveys typically utilize an unmanned aerial vehicle (UAV) to gather imagery, but UAVs have some notable drawbacks including government flight restrictions and inability to fly in poor weather (Casella et al., 2014; Gonçalves and Henriques, 2015; Long et al., 2016; Papakonstantinou et al., 2016; Scarelli et al., 2017). SfM surveys with imagery acquired using a camera mounted atop a pole can also produce good results, and such data collection is not subject to government regulation by the Federal Aviation Administration (FAA) and can operate in rougher weather (Gonçalves et al., 2016; Rossi, 2017; Wang and Watanabe, 2019; Weßling et al., 2013). However, the efficacy of pole photogrammetry is not as well documented as UAV-based methods. This study seeks to compare these two methods of image acquisition for SfM surveys of a beach to monitor beach erosion. These two platforms were used to conduct three monthly surveys of a beach, then compared and evaluated based on their relative performance and feasibility.

1.1 Coastal Erosion

Coastal erosion is a growing problem around the world, and the majority of US beaches experience significant erosion (The Heinz Center, 2000). Coastal erosion puts many people at increased risk from coastal hazards such as hurricanes, tsunamis, and winter storms. Erosion strains natural barriers, making them less effective and increasing the vulnerability of coastal communities. In areas like the US East Coast, human intervention to address erosion often takes the form of beach nourishment, the process of adding sand to a beach in an attempt to counter erosion and simulate natural accretion. Around the country, hundreds of millions of dollars are spent each year on beach nourishment (Smith et al., 2009); however, nourishment is only a temporary solution, and large amounts of sand can be swept away in a matter of hours during a large storm (Quartel et al., 2008). Healthy beach and dune systems are crucial for maintaining tourism-driven economies' protection from flooding and other coastal hazards (Giambastiani et al., 2007; Landry et al., 2003; Stockdon et al., 2012; Taylor et al., 2015). Monitoring the beach is

important to better understand erosion patterns and effectively protect coastal communities and maintain vulnerable beaches. Effective monitoring practices provide coastal managers and engineers with essential insight to the status of coastal erosion and mitigation projects.

Sandy beaches experience constant erosion and deposition, as ever-present tides and waves move sand around the beach (Houser et al., 2008; Inman et al., 1993; Mulhern et al., 2017; Quartel et al., 2008). General continuous erosion and accretion is driven by a balance of tides and waves, the relative strength of which produces distinct coastal features and beach characteristics (Mulhern et al., 2017). These processes of erosion and accretion follow seasonal cycles, with more erosion occurring during the winter months, and more accretion during the summer months (Inman et al., 1993; Masselink and Pattiaratchi, 2001; Quartel et al., 2008; Scarelli et al., 2017). Large storms, such as hurricanes and nor'easters can release tremendous amounts of energy on a beach and cause extreme erosion in a short time period (Houser et al., 2015, 2008; Quartel et al., 2008; Scarelli et al., 2017; Turner et al., 2016). Typical beach responses to storms include dune scarping (where the foredune face is cut away forming a sharp cliff), washout, and the formation of incised channels, overwash fans, and terraces (Morton and Sallenger, 2003). Beaches can also erode due to human activity. For example, stabilized inlets (those bound by jetties or other hard structures) are often a "hot spot" for beach erosion, as the jetties block the flow of sediment, starving downdrift areas of sediment (Galgano, 2007). Sea level rise is expected to accelerate coastal erosion and is already a leading cause of coastal erosion globally (Zhang et al., 2004). The East Coast of the US has a long trend of both beach erosion and sea level rise, with over a century of tidal gauge data showing sea level rise in the range of 20-40 cm over the 20th century (Zhang et al., 2004). Research has shown that small changes in sea level can have large impacts on erosion, especially in flat, low-lying areas. Over the long term, shorelines can retreat at up to 150 times the rate of sea level rise (i.e. 1 cm of sea level rise can lead to 1.5 m of shoreline retreat) (Leatherman et al., 2000).

Monitoring beach erosion is important to coastal managers, as they are charged with maintaining beaches and other coastal environments that communities rely on for protection and economic production. Even though coastal counties only make up 11% of US counties by number, they accounted for 18% of lost economic production due to natural hazards from 1990-2000 (Boruff et al., 2005). The combination of dense populations and vulnerability to hazards unique to the

coast (e.g., coastal flooding, hurricanes, storm surge, tsunamis), exacerbated by changing climate and sea level rise, makes the job of coastal zone managers extremely important. Recent storms have shown that coastal cities are vulnerable to significant damage and loss of life. Hurricanes Katrina and Sandy are etched into public memory by the scale of damage they caused as they hit large coastal cities. Coastal erosion only increases vulnerability to coastal hazards and can eventually lead to buildings and infrastructure being totally lost to the sea (Kim et al., 2017; Taylor et al., 2015).

1.2 Beach Monitoring

Existing beach elevation data primarily come from NOAA's Digital Coast and the USGS National Elevation Dataset (NED), which provide DEMs from aerial lidar scans flown over US coastal areas by the USACE, NOAA, and USGS. These datasets are generated from airborne lidar surveys, and provide good, free elevation coverage over the US, but not the rest of the world. However, lidar surveys are flown infrequently, so these data sources can only be used to monitor longer term trends, and typically do not provide adequate temporal resolution to monitor beach changes on an annual or finer timescale (Le Mauff et al., 2018). The NASA Shuttle Radar Topography Mission (SRTM) provides worldwide DEMs, but at a significantly coarser maximum resolution of 30m. SRTM is also no longer updated as the Space Shuttle program has been terminated, and SRTM has been shown to have significant error and bias in coastal areas, which can lead to extreme underestimations of the effects of coastal flooding and sea level rise (Gesch, 2018; Kulp and Strauss, 2016). Deep learning techniques applied to SRTM data present the latest solution to correct SRTM elevation and can reduce vertical RMSE by 50% in areas of diverse land cover (Kulp and Strauss, 2018). Other space-based alternatives include NASADEM, MERIT, and TanDEM-X, but these all suffer from a relatively low spatial resolution and are not continually updated to track changes in dynamic environments. SfM provides a solution for high resolution on-demand beach surveying, specialized in producing extremely high-resolution DSMs of specific areas (Eltner et al., 2016; Westoby et al., 2012). This also allows for highly customizable data acquisition, as surveyors have control over exactly when a survey is flown and can pinpoint an exact time in relation to tides or weather events to collect data.

UAVs provide a low cost and high-resolution method for monitoring coastal areas. They are a good alternative to the more expensive aerial lidar, but are more suited to smaller study areas, as flight duration and distance is limited by battery life and radio controller range, and government regulations mandate that the pilot must maintain direct visual contact with the UAV at all times (Gonçalves and Henriques, 2015; Le Mauff et al., 2018). Seasonal monitoring is very important, especially on beaches used heavily for tourism (Scarelli et al., 2017). As hurricanes and winter storms cause the most significant erosion of the year, coastal managers must have adequate monitoring information to plan and manage their sediment resources for the busy summer season, which UAV-based photogrammetry can provide (Inman et al., 1993; Masselink and Pattiaratchi, 2001; Quartel et al., 2008; Scarelli et al., 2017). UAVs can be deployed quickly, with little planning, allowing effective rapid response to storms that cause heavy erosion on sandy beaches (Turner et al., 2016). Turner et al. (2016) demonstrated this utility, showing that it can be an excellent tool in capturing the elusive immediate pre- and post-storm snapshots of the beach so desired by Quartel et al. (2008). Post-storm surveys are relatively easy to conduct, but pre-storm surveys require a system that can be launched on short notice to gather data before weather deteriorates and makes surveying impossible. Compared to older ground-based methods, UAV data are both higher resolution and more easily obtained (Mancini et al., 2013; Turner et al., 2016).

1.3 Structure from Motion

Structure from Motion (SfM) is a revolutionary technique in photogrammetry that can be implemented using off-the-shelf equipment and software and without photogrammetric expertise. SfM identifies matching points in overlapping images to automatically and simultaneously calculate camera pose and position and the location of that point in a 3D space (Snavely et al., 2008; Ullman, 1979). This photogrammetry technique has been well documented as an excellent tool for generating 3D topographic reconstructions (Eltner et al., 2016; Fonstad et al., 2013; James and Robson, 2012; Westoby et al., 2012). SfM matured in the 2010s, and there are now many excellent software applications for processing imagery into point clouds (Eltner et al., 2016). Because a priori camera pose and position is unnecessary, virtually any camera can be used, unlike earlier photogrammetric methods (Westoby et al., 2012). However, accurate reconstruction does depend on images with a sufficient amount of overlap (at least 70%) and a

variety of camera look angles and positions (James and Robson, 2014; Westoby et al., 2012). As the name implies, image sets are typically gathered using a camera in motion, often using a drone to gain an aerial perspective (e.g., Gonçalves and Henriques, 2015; Harwin and Lucieer, 2012; Mancini et al., 2013; Scarelli et al., 2017; Taddia et al., 2020; Turner et al., 2016), but can also be collected from a terrestrial platform (e.g., Castillo et al., 2012; James and Robson, 2012; Pikelj et al., 2018; Rossi, 2017; Wang and Watanabe, 2019; Weßling et al., 2013; Westoby et al., 2012).

As the commercial drone industry has exploded within the past decade, so has the use of UAVs for topographic surveying (e.g., Gonçalves and Henriques, 2015; Harwin and Lucieer, 2012; Mancini et al., 2013; Scarelli et al., 2017; Taddia et al., 2020; Turner et al., 2016). UAVs offer an excellent platform for aerial photography, with many low-cost systems that are ready to use for SfM surveys directly off the shelf (Turner et al., 2016). Their ease of operation and deployment has made them a popular choice for researchers seeking a high spatial and temporal resolution set of elevation data of relatively small sections of beach (Casella et al., 2014; Gonçalves and Henriques, 2015; Harwin and Lucieer, 2012; Long et al., 2016; Mancini et al., 2013; Papakonstantinou et al., 2016; Scarelli et al., 2017; Taddia et al., 2020; Turner et al., 2016). UAV surveying typically requires three components: the drone itself and flight controller, post processing software suite, and a set of ground control points (GCPs) to precisely georeference the resulting point cloud in a coordinate system. However, with the advent of small RTK-GNSS systems that can be mounted on a drone, external GCPs may not be necessary, thus making the survey process much more streamlined (Taddia et al., 2020).

However, UAVs and SfM suffer from some errors and limitations. In coastal surveying, measuring nearshore bathymetry is necessary to paint a full picture of the beach (Holman et al., 2013; Quartel et al., 2008), but SfM can only measure the “dry” beach down to the runup zone (Mancini et al., 2013; Turner et al., 2016). It is possible to measure water depth with SfM by compensating for light refraction when reconstructing the seabed, but this requires clear water, little to no wave activity, and sufficient structure on the bottom (Dietrich, 2017; Kasvi et al., 2019; Slocum et al., 2019). Unfortunately, these requirements make SfM-based bathymetry impossible in a beach environment with turbid water, constant wave action, and little to no bottom structure. A possible solution is to derive bathymetry from surface waves but this

requires a drone capable of recording long-dwell time series imagery and is an indirect measurement and significantly worse in resolution and reliability (Brodie et al., 2019; Holman et al., 2013). Resulting point clouds from SfM provide good elevation data and reconstructions when done well but are often more fuzzy and less precise than similar scans done with lidar. Occasionally, there can also be breaks or "ghosting" in the point cloud. When viewing a point cloud, a single, solid object such as the beach surface appears as a double image, where the same object is reconstructed multiple times in vertically offset layers. When seen as a cross section, what should appear as a single surface can appear as multiple layers. Ghosting inhibits the generation of accurate DSMs, as it is unclear which is the "true" surface. Ghosting is caused by insufficient overlap, poor camera calibration or a combination of the two. Using poorly calibrated digital camera models, with incorrect focal length and radial and tangential distortion parameters can result in a "doming" effect in the DSM, where the reconstruction is curved (typically convex), resulting in a positive elevation bias in the center of the DSM, gradually shifting to a negative bias towards the edges, or vice versa (James et al., 2020; James and Robson, 2014). Both ghosting and doming can be seen in Figure 1. The rolling shutter effect, caused by using a camera sensor that record each row of pixels sequentially rather than simultaneously, can worsen the doming effect. Because SfM relies on finding matching points in multiple images taken at different times, reconstruction of moving surfaces such as waves is impossible. However, these errors can be mitigated by using higher quality cameras as well as accurate digital camera models and imagery with sufficient resolution, overlap, and variety of look angles (Eltner et al., 2016; James et al., 2020; James and Robson, 2014). Ground control points will also alleviate doming, and are necessary to accurately georeference the resulting DSM and point cloud, unless using a UAV with an onboard high accuracy RTK-GNSS reciever (James and Robson, 2014; Taddia et al., 2020).

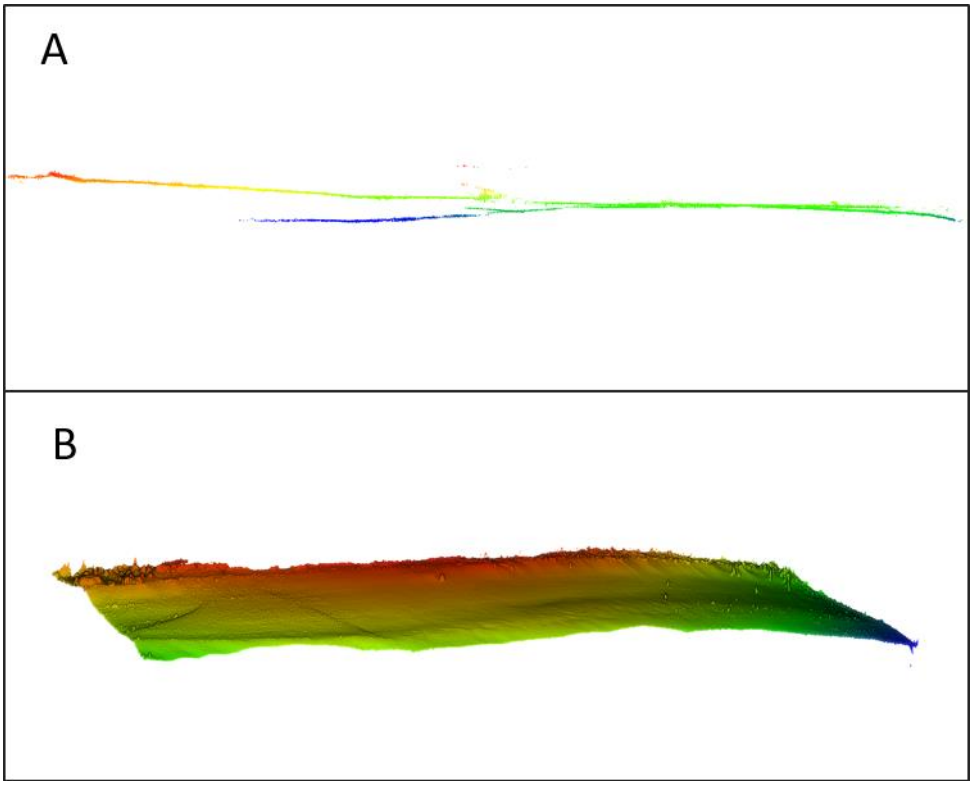

Figure 1: A: cross section of a pole photogrammetry point cloud. The dune ridge is on the left, and ghosting appears on the right where multiple surfaces are produced rather than one.

1.4 Pole Photogrammetry

Although UAVs are the dominant platform for SfM topographic surveys, removing the drone from the equation offers a solution when UAV flight is not possible or practical. Terrestrial photogrammetry utilizes the same SfM workflow as UAV SfM, but images are gathered from the ground rather than the air. To achieve an aerial perspective similar to that of a drone, a pole can be used to elevate a downward-facing camera, often a small wide-angle lens action camera to achieve a wide field of view and maximize the surveyable area (Gonçalves et al., 2016; Rossi, 2017). For example, Rossi (2017) demonstrates the utility of pole photogrammetry in canyons, where steep walls can prove an obstruction for flight, and sinuous stream paths may disrupt line of sight with a drone. Terrestrial approaches can provide good results, as long as the image set contains a sufficient diversity of perspectives to build a full reconstruction (e.g., Castillo et al., 2012; Eltner et al., 2016; Gonçalves et al., 2016; James and Robson, 2012; Rossi, 2017; Wang and Watanabe, 2019; Weßling et al., 2013; Westoby et al., 2012). Scans can be conducted either

along a single walking path, or multiple parallel transects for areas wider than what can be covered in a single pass (Gonçalves et al., 2016). Because pole photogrammetry is operated from the ground, it solves two critical limitations of UAV photogrammetry: government flight restrictions and weather limits. In coastal environments, surveyors may often encounter high winds or other poor weather conditions (especially for rapid-response post-storm surveys), as well as crowded areas which require a waiver from the FAA to fly over.

Pole photogrammetry enjoys the same or greater ease of use as UAV SfM, while benefiting from lower equipment and training costs and greater flexibility in planning and conducting surveys. A DJI Mavic 2 Pro, as used in this study costs $1,600, while a GroPro Hero8 and telescoping pole costs $360. The primary drawback of pole photogrammetry is that the camera is at a much lower altitude, decreasing the area included in a single image. Previous studies typically use a pole of 4-5 m, carried roughly a meter above the ground for a total camera height of 5-6 m (e.g., Gonçalves et al., 2016; Rossi, 2017; Wang and Watanabe, 2019), while a UAV SfM scans commonly fly at an altitude of 40-60 m, with a government mandated maximum altitude of 400 feet (~120 m) above ground level in the US (Mancini et al., 2013; Scarelli et al., 2017; Turner et al., 2016). This necessitates more passes to cover the same area and combined with the functionally necessary slower speed of travel results in longer times to scan the same area. In addition, Gonçalves et al. (2016) note that the smaller area covered in each photo requires larger image set, leading to significantly longer processing times. However, low altitude and slow speed can potentially result in higher resolution and more detailed surveys. Considering longer image acquisition and processing times, combined with potentially higher resolution, it follows that pole photogrammetry can be especially well-suited to applications with a smaller area of interest and where high resolution is desired. For example, Wang and Watanabe (2019) show the efficacy of pole photogrammetry for monitoring erosion impacts on campsites from overuse, and Weßling et al. (2013) use pole photogrammetry for documenting archeological sites. Pole photogrammetry is also not reliant on UAV battery life which typically last about 20-30 minutes, so longer scans are possible without pausing to change batteries.

2. Methods

2.1 Study Area

The study area is an approximately 200 m x 100 m (2 ha) stretch of beach near the southern end of Capers Island, South Carolina, approximately 13 miles north-east of Charleston. The island is an uninhabited barrier island dominated by salt marsh and maritime forest, with a beachfront that experiences a mix of accretion and deposition, shaped primarily by waves and tides. The last major erosion event to affect the island was Hurricane Hugo, a Category 4 storm that made landfall roughly 10 miles southeast in September 1989. The shoreline of Capers Island retreated an average of 29 m during this storm (Sexton and Hayes, 1991). Since Hugo, the island has been relatively stable, with minor seasonal erosion and deposition cycles and longer term (4-7 year) cycles dictated by the behavior of neighboring inlets (Fitzgerald, 1984). Sediment along Capers Island and the neighboring coastline is generally north to south and has likely been this way for at least 300 years (Fitzgerald, 1984). Sexton and Hayes (1991) state that the island is a regressive barrier island, although satellite photography since Hugo suggests a transgressive trend. This island was selected for study because it is unpopulated and thus free from large beach crowds and other inhibitors to UAV flight and represents a natural barrier island subject to exclusively natural sediment forces. The particular stretch of beach used for this study is just to the north of Capers inlet, where the ebb tidal delta forms and affects sediment budgets for the more populated islands to the south.

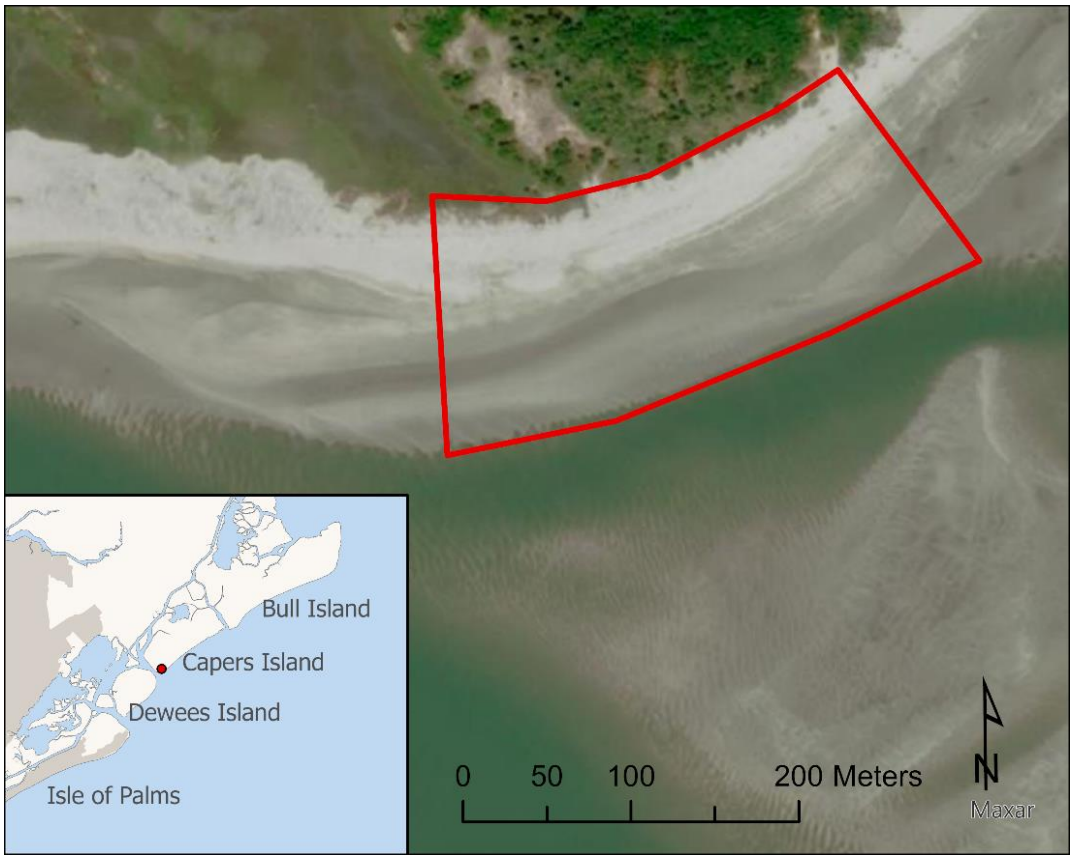

Figure 2: The study area at the southern end of Capers Island. Note the channel that runs between the study area and offshore sandbar.

2.2 Materials

DJI Mavic Pro 2 drone was used for all aerial photogrammetry. This UAV uses a Hasselblad L1D-20c camera stabilized by a three-axis gimbal. The L1D-20c camera has a 35mm equivalent 28mm perspective lens, and a 20 megapixel 1 in CMOS sensor (5472 x 3648 pixels). The UAV is controlled by a DJI controller, which can interact with a mobile device and/or headset to control flight, camera, and provide a first-person view using the drone's onboard camera. Flight planning and execution was done using the Pix4Dcapture app for Android, which can plan flight path (e.g., single grid, double grid, circular, etc.), altitude, camera angle, image overlap, and speed. A 128 GB microSD card was used to store images. A total of six batteries were used, each providing roughly 20 minutes of flight time depending on wind conditions. One survey flight was flown per battery. The Mavic Pro 2 has an onboard GPS and altimeter which are used for flight control and geotagging image files in both EXIF and XMP metadata. Three-axis

orientation information for both the craft and the gimbal is also embedded into each image's metadata via XMP tags.

Figure 3: DJI Mavic Pro 2 and Emlid RS2 GNSS base station.

Figure 4: Pole photogrammetry system.

The pole photogrammetry system consisted of a lightweight aluminum 12 ft (~3.5 m) telescoping pole carried by hand. The GoPro Hero8 Black camera was mounted at the top, approximately 5 meters above ground level at a slightly oblique angle of about 10° above nadir. The GoPro Hero8 has a 1/2.3 in 12 megapixel sensor (4000 x 3000 pixels), and a 2.92 mm (16.4 mm equivalent) fisheye lens for a horizontal field of view of 122.6° and a vertical field of view of 94.4°, as well as an onboard GPS receiver to automatically embed geolocation information into the image files. The GoPro battery life is exceptionally good in comparison to the drone batteries and does not need to be changed to complete an entire survey. Images were saved to a 128 GB microSD card. Because there is no software to set image overlap, calculations and preliminary tests were done to determine at what time interval images should be taken and how widely spaced adjacent passes should be. It was found that setting the GoPro's time lapse setting to take a photo every 0.5 s provided over 90% vertical overlap between sequential images and spacing each subsequent transect by 4.5 m would provide a sufficient side overlap of roughly 70%. All SfM processing was done using Pix4Dmapper. Point cloud comparisons were conducted in CloudCompare, and DEMs of Difference (DoD) were evaluated in ArcGIS Pro. GNSS-ground truth surveys were conducted using Emlid Reach RS+ and RS2 RTK-GNSS units and 2 m survey poles, corrected using a CORS station at Fort Johnson, SC, approximately 22.5 km from the study site.

Three lidar DEMs were downloaded from the National Oceanic and Atmospheric Administration's (NOAA) Digital Coast portal. These DEMs were generated from lidar surveys flown in 2016, 2017, and 2018. The 2016 and 2018 DEMs used a topobathy lidar, which measures both terrestrial elevation as well as shallow water bathymetry, while the 2017 DEM used a standard terrestrial lidar sensor. All DEMs were 1 m in resolution and were not tide controlled. Lack of tide control is not an issue for topobathy surveys, as the sensor used seamlessly measured elevation in land and water, but may restrict the area observable by the standard lidar. Three additional lidar datasets were downloaded from 2010, 2006, and 1997. As DEMs were not available for these flights, digital surface models (DSMs) were used instead. Due to drastic changes in the beach over this longer time period, these datasets did not provide useful elevation data for calculating erosion on the beach face but are useful for measuring overall shoreline retreat.

2.3 Field Surveys

Three survey campaigns were conducted on the dates of September 18th, October 13th, and November 16th, 2020. This time interval was chosen as it is a reasonable period to track seasonal beach changes, and also spans the peak of the Atlantic Hurricane Season when storms are most intense and most frequent. Survey campaigns were timed to be conducted at or near the peak of the tide cycle, with all imagery taken at low tide to maximize the surveyable beach area. Drone imagery was taken at a variety of altitudes, patterns, and camera angles, to ensure a good mix of oblique and nadir imagery at different altitudes as recommended by Eltner et al. (2016) and James and Robson (2014). The lowest flights were flown at 50 m above ground level (AGL) to give abundant clearance over nearby trees, and the highest were flown at 115 m AGL to stay within the FAA's mandated ceiling of 400 ft.

The September survey campaign was conducted on September 18th, 2020, after waiting several days for poor weather to clear. Upon arriving at the beach, the RS2 base station was set up and powered on. Protocol developed for the study indicated that the pole photogrammetry and RTK-GNSS surveys would be conducted first, then lastly fly the UAV surveys. However, weather was forecasted to deteriorate throughout the day, so UAV flights were flown before pole photogrammetry and GNSS surveys as the drone is dependent on low wind speed and good visibility. A total of four flights were flown, the first a single grid at 115 m and 85° camera angle, second a double grid at 50 m and 80°, third a single grid at 50 m and 80°, and the fourth a single grid also at 50 m and 80° to cover some area missed by the third flight.

The pole photogrammetry survey was conducted using single-grid approach, with a row spacing of approximately 4.5 m to ensure about 70% side overlap (sidelap), and the camera set to take a photograph every half second. The camera angle was set to approximately 80 degrees, although it is not gimbal stabilized, so there is some slight variation in camera angle throughout the survey. The survey was conducted at a brisk walking speed of about 1.5 m/s and consisted of roughly 6,000 images taken in 21 transects parallel to the beach. The RTK-GNSS survey was taken with the Emlid RS+ unit and 2 m survey pole, with a thread adapter that increased the antenna height to 8.65 cm. The GNSS survey was taken simultaneously with the pole photogrammetry survey points were taken 6 m apart from one another in three transects

perpendicular to the beach from the foredune foot to just below the runup zone. Points were collected for one minute with the highest available RTK GNSS precision ("FIX" status), with 6 m spacing between sequential points, generating 60 points total.

October and November survey campaigns were conducted on October 13th and November 16th, respectively. The survey workflow was similar to September, but UAV surveys were conducted following, rather than preceding pole photogrammetry and RTK-GNSS surveys which used the exact same surveying parameters as in September. In October, drone flights were flown with similar parameters as September, but at altitudes of 50 m, 100 m, and 110 m and with slightly more oblique camera angles of 70°-80° in an attempt to rectify doming issues encountered in preliminary processing of the September data. November flights were planned with similar altitudes, but with a wider variety of camera angles ranging from a very oblique 40° flight to nadir flights.

2.4 Data Processing

All photogrammetric processing was completed in Pix4Dmapper, a commercial SfM-based software application for generating 3D maps and models with survey-grade accuracy. The photogrammetric workflow is broken into 3 steps. Step 1 consists of extracting and matching keypoints in images, which form the basis of the reconstruction, camera model optimization, and geolocation. A good result in Step 1 is crucial to ensure a quality point cloud, DSM, and orthophoto. After Step 1 is finished, results can be improved by adding manual tie points and/or ground control points, which can repair errors in the reconstruction and geolocate the model more accurately than the onboard GPS information embedded in images. However, if a camera is paired with an accurate RTK-GNSS, such as the DJI Phantom 4 RTK, adding GCPs is not necessary for accurate geolocation, and Pix4D includes an Accurate Geolocation pipeline to utilize this information which significantly reduces processing time (Taddia et al., 2020). Step 2 uses the keypoints found in Step 1 to produce a densified point cloud and 3D mesh surface. Finally, Step 3 generates a DSM, orthophoto, and optional reflection and index maps.

The pole photogrammetry surveys consisted of 6,000-8,000 images each, taken every 0.5 s in roughly 20 transects. Tests showed that the use of every image resulted in an unnecessarily high overlap, and good results could still be produced using only every third image (taken every 1.5

s). This did not significantly decrease resolution or accuracy, while dramatically reducing processing time, so only every third image was used. The project was initiated using the "3D maps" processing profile and using geolocation information embedded in the Exif data by the GoPro. However, the GPS error in the z-axis was large (2-5 meters) compared to the overall elevation difference of the study area (~2.5 meters). In combination with the low collection height (5 meters AGL), this error significantly degraded the quality of reconstruction by preventing good calibration of the images. To compensate for this issue, the elevation values were replaced with estimations based on the RTK GNSS survey. Each image was sorted into one of 20 transects, then images in each transect were assigned a new altitude assuming an even slope from the foredune to waterline. This produced quality results after Step 1, and any altitude inaccuracy would be corrected later by adding ground control points. With the estimated altitudes loaded, altitude accuracy was set to 1 m, as this proved to eliminate curvature error in the reconstruction ("doming") nearly entirely, as well as to significantly reduce the appearance of multiple disconnected reconstructed surfaces ("ghosting"). The default camera model in Pix4D for the GoPro Hero 8 produced very severe doming, as described by Eltner et al. (2016) and James and Robson (2014). This camera model is incorrectly categorized as a perspective lens, while the GoPro uses a fisheye lens. Therefore, the camera model was modified to correctly represent the fisheye distortion of the camera, using the same parameters as digital camera models used for earlier GoPro versions which appear to use an identical lens and sensor. Step 1 was then run using ½ image scale, free flight or terrestrial, rematch box checked, and all other settings set to default.

Once Step 1 was finished, manual tie points (MTPs) were added, then the project was reoptimized to fix any breaks or ghosting. MTPs involve the marking of specific features in overlapping images and can improve reconstruction quality in difficult environments. Additional MTPs were added until either all issues were fixed, or the addition of more MTPs had no more positive effect, which was typically achieved between 20 and 100 MTPs, with each point marked in 20 or more images. After MTPs were added, GCPs were marked. Marks in the sand from the RTK survey pole were used for GCPs and proved to be a very reliable and easily discernible marker. In all surveys, pole photogrammetry and RTK surveys were conducted simultaneously, with the RTK survey being started a few minutes before pole photogrammetry enabling more marks to be included in the pole imagery. Similar to MTPs, GCPs were marked in as many

images as possible, typically 20 or more. Around 20 GCPs were marked throughout all projects, well dispersed throughout the survey area. The results were reoptimized again after marking GCPs. Following the conclusion of Step 1 processing, Step 2 was run using original image scale, classify point cloud on, 3D mesh turned off, and all other setting left to default. Step 3 was run with raster DSM on, grid DSM to LAZ, raster DTM on, and all other settings default.

UAV Pix4D projects for each survey campaign included all images taken from all flights, around 800-1,000 images total. Projects were also initiated in 3D maps mode, using embedded geolocation information, which includes camera orientation data in addition to X, Y, Z geolocation coordinates. Settings for all drone projects were identical to pole photogrammetry settings for all three processing steps. However, projects did not require the use of MTPs. To correctly mark GCPs, both UAV and pole imagery were run together in a single project through Step 1. MTPs, GCPs, and corresponding marks were imported from the pole photogrammetry project, and results reoptimized. Because the UAV and pole imagery yielded two separate surfaces, a few more (roughly 8) MTPs were added to sync these two surfaces. Results were reoptimized again, then GCP marks were added to the drone imagery, using the same marks from the RTK survey pole which were again clearly visible in the imagery, and reoptimized again. The GCPs and marks were then imported into the UAV imagery project, and reoptimized. However, because the UAV flights were conducted before the RTK-GNSS survey, GCPs were not able to be marked in September drone imagery. Instead, after the UAV and pole photogrammetry surfaces were synced, several MTPs were exported as GCPs and imported to geolocate the UAV project. Steps 2 and 3 were then run as in the pole photogrammetry projects.

To eliminate any remaining inconsistencies in DSM georeferencing, resulting DSMs were adjusted using the ArcGIS Georeference module, to slightly adjust the position of DSMs and minimize error due to inaccurate georeferencing. The November DSM was used as the “master” to which the September and October DSMs were adjusted to match. Stationary landmarks such as trees were used to visually align the DSMs, then a gradient descent was performed, iteratively adjusting DSM position to minimize the mean absolute difference between the two DSMs. Inaccuracy in the vertical direction was corrected by adjusting the elevation values of the September and October DSMs with the Raster Calculator, once again using the November DSM as the master. Elevation difference in the backdune area, which should show little change from

month to month, was used to estimate vertical corrections, then a similar gradient descent was performed to minimize the mean absolute difference between DSMs.

As is common in SfM reconstructions, point clouds typically contained erroneous points. In order to remove stray points, the cloud was loaded into CloudCompare, a powerful and free application for visualizing and processing point clouds. The cloud was initially trimmed using the cross-section tool to remove most large and obvious outliers, then filtered using the noise filter on default settings. To eliminate instances of "ghosting" prevalent in Pole Photogrammetry point clouds, where the resulting point cloud produces two or more surfaces in the same area, the lasthin tool from LAStools was used to select only the median points, then a raster DSM was generated in CloudCompare.

2.4.1 DEM of Difference

To track changes in output surface models (DSMs), ArcGIS Pro was used to generate a DEM of Difference (DoD). A DoD is generated by computing the difference between sequential DEMs to quantify where elevation has increased or decreased and is a commonly used metric in geomorphic change detection surveys (e.g., Brasington et al., 2003; James et al., 2012; Le Mauff et al., 2018; Rossi, 2017; Scarelli et al., 2017; Vaaja et al., 2011; Westoby et al., 2012). To generate a DoD, two sequential DSM rasters were loaded into ArcGIS, then the first DSM was subtracted from the second using the Raster Calculator tool. Areas that did not reconstruct (e.g., the runup zone) were clipped out to avoid noise from poor results. By subtracting the earlier DSM from the later DSM, areas with a positive value in the DoD indicate accretion, where beach elevation has increased, and negative areas indicate erosion, where elevation has decreased. DoD analysis was used to quantify change from month to month in this survey, as well as compare the beach state to historical states recorded in lidar data.

DEM of Difference was also used to compute differences in Pole and UAV surveys from the same months. In this case, georeferencing beyond applying GCPs was not necessary, as both Pole and UAV surveys from the same month were georeferenced using identical GCP sets. Pole photogrammetry DSMs were subtracted from the drone DSMs, with a higher value in the DoD indicating areas where the UAV measured a higher elevation, and vice versa. For a bare beach

such as this, there is no practical difference between the DSM and a DEM, as the bare sand of the beach does not require any ground filtering, as it is the only surface present.

Finally, DoD was used to calculate differences between the November drone survey (the final state of the beach in this study) to DEMs generated in from lidar surveys flown in 2016, 2017, and 2018. In earlier datasets, the makes up the present beach was forested, and thus doesn't provide relevant elevation information to generate a DoD. However, these datasets, generated in 1997, 2006, and 2010 do provide valuable information to measure shoreline retreat over this longer time period. This was done by measuring the distance from the historic to present foredune foot, as the waterline observed in these datasets varies based on the tide level, and none of the lidar datasets used here are tide controlled. Therefore, the foredune ridge serves as a good stationary landmark to gauge shoreline retreat.

2.5 System Evaluation

UAV and Pole photogrammetry were compared to one another to evaluate their relative performance, resolution, and feasibility. Resolution was evaluated by finding the maximum resolution point clouds and orthophotos produced by each system. Feasibility was evaluated in terms of cost and difficulty to complete a survey. Cost evaluations included equipment and training costs, as well as the total time and other resources needed to complete a survey. Difficulty to complete a survey was evaluated based on necessary expertise to complete a survey and any legal or environmental restrictions that may be encountered in a beach environment.

3. Results

3.1 Feasibility

The UAV system used in this survey is significantly more expensive than the pole photogrammetry system. A new DJI Mavic Pro 2 costs $1600, and a smartphone or tablet is necessary to plan and execute flights. Additional batteries cost $150, putting the total cost of the system at $3100. In addition, the FAA Part 107 exam costs roughly $150, and time and study materials are necessary as well. UAV surveys are much easier conduct but do require training and knowledge of flight regulations, as well as experience with operating the UAV to be able to fly safely and effectively. Given proper flight planning, conducting surveys is very simple using

an application such as Pix4Dcapture, as the UAV will fly a mission autonomously, and the pilot only needs to monitor the system should anything go wrong. This also allows for easy, routine repetition of the exact same flight plan. For larger areas, the greater speed of the UAV is a major advantage, allowing much larger areas to be surveyed during the limited amount of time available at low tide. Fewer images are needed since the higher altitude means greater image overlap; this also shortens processing time. Few problems were encountered in data processing expect for mild doming, potentially caused by the rolling shutter effect, rectified by reducing the vertical accuracy threshold of the camera positions and adding ground control points (GCPs).

The pole photogrammetry system is far less expensive than the UAV. The camera and pole together cost $380, $320 of which is the camera alone. In addition, no formal training or certifications are required to operate the equipment. Due to the smaller area covered in a single frame or swath, and relatively slow speed, pole photogrammetry surveys take much longer to perform. A single drone flight over this study area (2 ha) can be completed in less than 15 minutes and produce good results, while a pole photogrammetry survey takes well over an hour (approximately the same time as the RTK-GNSS survey) and requires walking approximately 7.5 km. In addition, the larger image sets from pole photogrammetry take much longer to process in Pix4D and requires significantly more expertise with the software to produce good results. Many more issues were encountered in processing, such as doming and ghosting. Doming, described by Eltner et al. (2016) and James and Robson (2014) results in a DSM with a persistent curvature, where an ideally flat surface is higher in the center and lower towards the edges, or vice versa. Ghosting results in a “double image”, where the same surface is generated twice at different offsets and orientations, making it difficult to discern which surface truly represents the target surface. This can be seen in Figure 1, where a single surface is reproduced multiple times. However, the freedom from flight and weather restrictions is a benefit, as is the very low cost of equipment and training. Conducting the survey itself is as simple as turning the camera on, starting a timelapse, mounting it to the pole, then walking in a grid pattern.

Both systems benefit from powerful computing resources, especially a GPU with Nvidia CUDA cores. A machine with recommended system specs for this scale of project costs upwards of $2000. Software is also quite expensive, as a commercial license for Pix4Dmapper software costs $291 per month, or $5000 for a perpetual license. Open-source alternatives for SfM

reconstruction (e.g., OpenDroneMap) are available, however. Processing time is heavily dependent on settings, especially the resolution of the DSM and orthophoto. However, the pole photogrammetry imagery can take nearly twice as long as the drone imagery to complete Step 1 using identical settings. Steps 2 and 3 show little difference if settings (especially resolution) are identical.

3.2 DSM Quality

October and November UAV photogrammetry surveys produced high quality DSMs, while the September survey showed significant doming, thus obscuring the true beach elevation. DSMs for this study were produced at 5 cm resolution, but it is possible to generate DSMs and orthophotos approaching 1 cm resolution. October and November DSMs do not present any issues with doming or ghosting and excellently show elevation across the study area. Due to the inclusion of high-altitude imagery, the DSMs and orthophotos both include a much wider area than that covered by the pole photogrammetry survey.

Pole photogrammetry surveys produced far poorer results, retaining numerous artifacts from the photogrammetry process. Most notable is the prevalence of ghosting, where the ground surface is incorrectly reproduced as two or more separate surfaces (Figure 1). Despite attempts to remove erroneous points from point clouds using noise filtering algorithms, manual segmentation, and generating a DSM using only median points, this problem persisted in pole photogrammetry reconstructions from all three months. These artifacts make it impossible to discern the true elevation from resulting DSMs. Ghosting appeared to be worse on certain types of beach surface. Areas with few features (e.g., driftwood, seashells) or a tight, rippled surface were very difficult to reconstruct, and resulted in complete failure of some sections of the beach to reconstruct. Issues with ghosting can often be fixed by adding MTPs after running Step 1 of Pix4D, but the uniform nature of the beach surface can make it extremely difficult to mark MTPs if no easily identifiable features appear in the images. While artifacts appear throughout the DSM, they were less severe closer to the dunes, where there are larger variations in elevation as well as logs and mats of reeds deposited by the tides.

Pole photogrammetry surveys can generate DSMs and orthophotos with sub-centimeter resolution, as fine as 3 mm. This is extremely fine, especially for a study such as this where 5 cm

resolution is sufficient. Producing such fine resolution products also results in unnecessarily large file sizes, demanding large amounts of memory for any application to handle, making them unfeasible for a study area of this size. The software can, however, be set to export specific (e.g., 5 cm) resolution outputs.

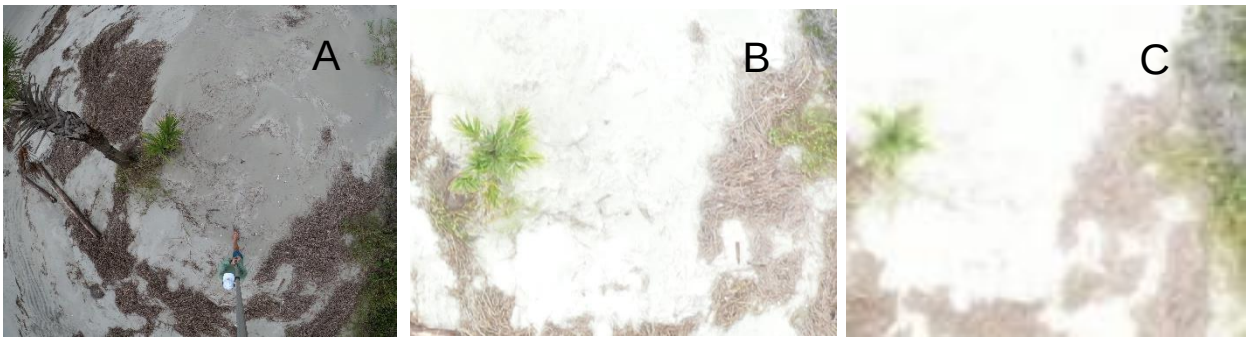

Figure 5: Pole photogrammetry image (A), and 50 m altitude (B) and 110 m altitude (C) drone photos cropped to the same area. Surveys from the pole photogrammetry can produce DSMs and orthophotos of up to 3 mm resolution, while 50 and 110 m drone photos can produce 1.25 cm and 3 cm resolution products, respectively.

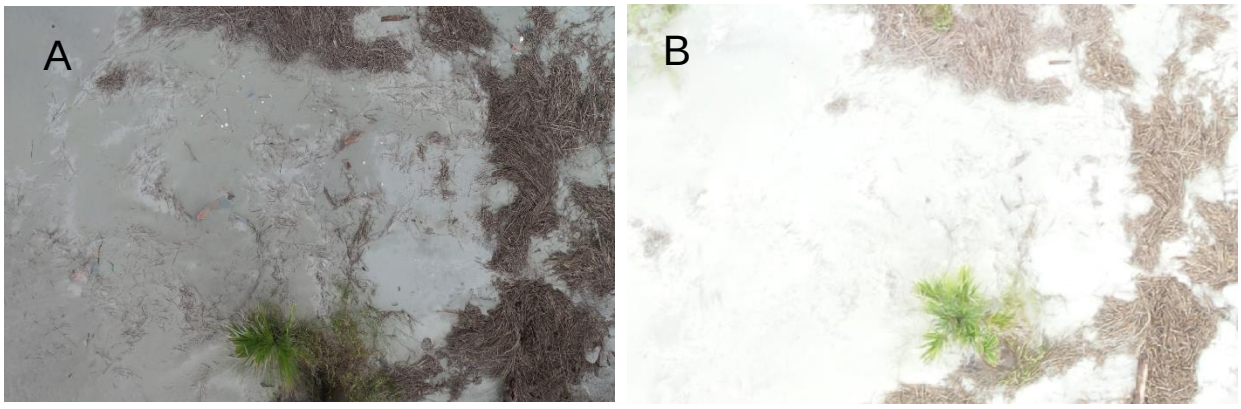

Figure 6: Pole photogrammetry orthophoto at 0.3 cm resolution (A), and drone orthophoto at 1.25 cm resolution (B).

3.3 Orthophoto Quality

Orthophoto resolution depends on the camera resolution, field of view, and distance from the ground. Both systems use a high-resolution camera, but because the GoPro used in pole photogrammetry is so close to the ground, it can produce extremely fine resolution orthophotos,

as fine as 3 mm per pixel. Resolution of drone orthophotos depends largely in altitude. Lower flights at 50 m altitude can produce results up to 1.25 cm in resolution, while flights approaching the FAA's approximately 120 m ceiling can produce orthophotos of roughly 3 cm resolution when using nadir or slightly oblique imagery. When using imagery from flights of varying altitude, maximum resolution matches that of the lowest altitude flight.

The UAV imagery produced good quality orthophotos, with similar georeferencing issues to the DSMs, although no elevation correction is necessary. From month to month, there is a slight difference in color saturation and temperature, likely due to differences in lighting. The September campaign took place on an overcast day and produced a cooler and more saturated orthophoto than October and November which were done in full sunlight. Some artifacts or black spaces do appear, but these are all in the water where photogrammetry is known to perform poorly or on the fringes, outside the area of interest. The pole photogrammetry orthophotos show numerous artifacts, as seen in Figure 7. Most common were clear seams between transect and instances where the operator is seen in the orthophoto (though image masks can additionally be used to remove artifacts of this kind). In addition, the GoPro's automatic white balance shifted throughout the survey, resulting in areas that are notably warmer than the rest of the image. The orthophotos perform best near the dunes and the water's edge.

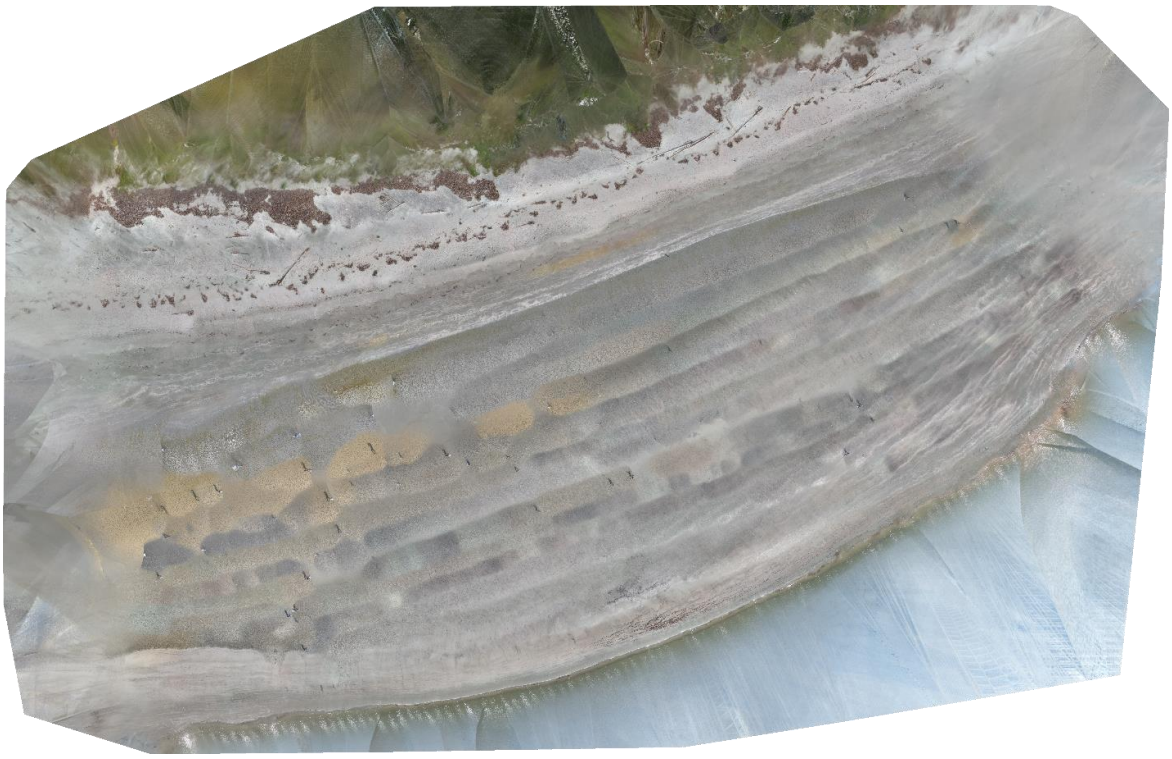

Figure 7: Incompletely processed October pole photogrammetry orthophoto, showing seams between transects, white balance variations, and numerous appearances of the operator.

3.4 Monthly Beach Change

Intractable doming present in the September DSMs made elevation comparisons between the September DSM and other months impossible, as DEMs of Difference showed mainly artifacts rather than true difference. Similarly, artifacts in pole photogrammetry DSMs rendered them useless for subsequent elevation analysis. However, the drone DSMs for October and November worked well to show changes int the beach surface. Between October and November, the most pronounced changes in elevation occurred in the central and northeastern sections of the study area. The northeastern portion of the beach was the narrowest and steepest part in the October survey, but by November the beach had widened, and the slope became more gradual, resulting in an increase in elevation in this section. Conversely, the central section showed a decrease in elevation. While the overall beach width changed little here, the area near the shoreline was vertically eroded by roughly a meter, with a distinct wavy pattern, perhaps as the result of a change in tidal currents due to a shift of the offshore ebb tidal delta. The central section continued to show erosion further up the beach to the foredune foot, which showed some mild

scarping, as seen in Figure 10. Further to the southwest, the DoD showed a mix of erosion and deposition, with 4 alternating sections showing roughly 10 cm of erosion and deposition between the shoreline and foredune foot.

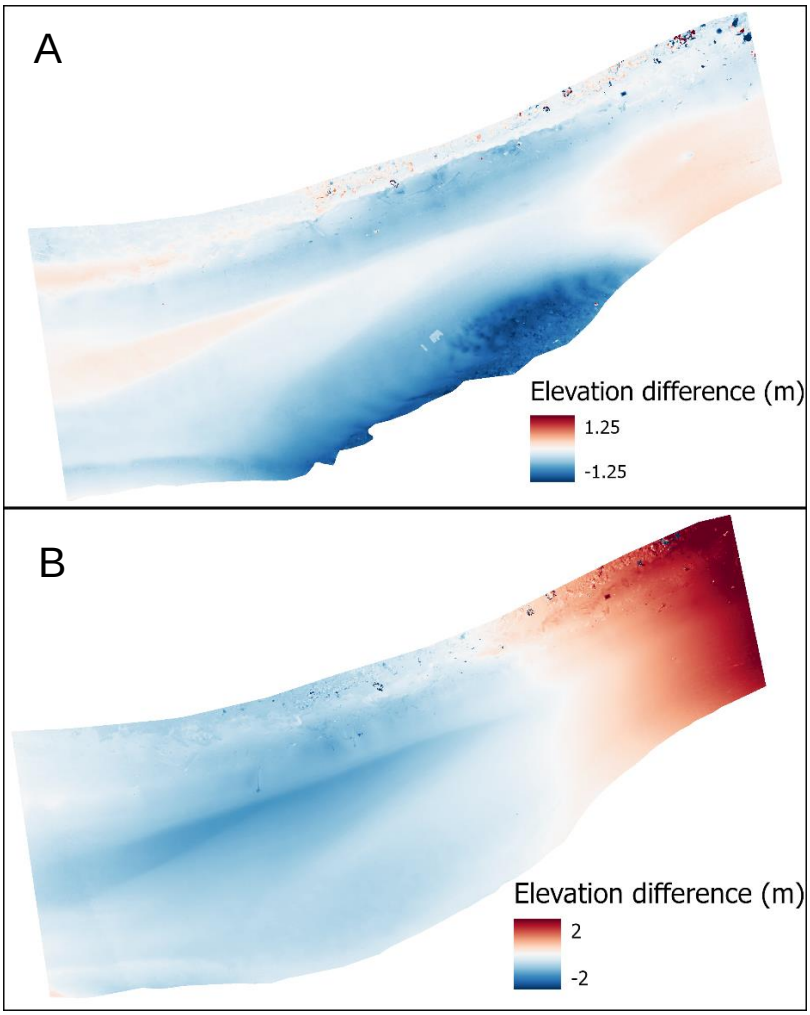

Figure 8: DEMs of Difference generated from UAV imagery. Change from October to November (A) shows a mix of erosion and accretion, while the September to October DoD (B) only shows doming present in the September DSM.

In orthophotos, changes in overall beach shape can clearly be seen. In September, the beach retains a relatively even width across the study area, while in October, the beach rapidly narrows in the northeastern third of the image, with a slight bulge in the central portion. Also visible is a shallow tide pool, up beach of the berm which appears as a dark stripe that is not present in the other orthophotos. By November, the beach remains narrow in the northeast, but has widened

somewhat. Most notable is erosion in the central portion, where the channel incised an indentation into the shoreline. Measuring from the foredune foot to the waterline, the narrowest point in November was 51 m, and the widest 134 m. In October, the narrowest and widest were 69 m and 121 m respectively, and 118 m and 93 m in September. In all three months, the widest point was towards the southwest portion of the beach, while the narrowest was in the northeast or central portion.

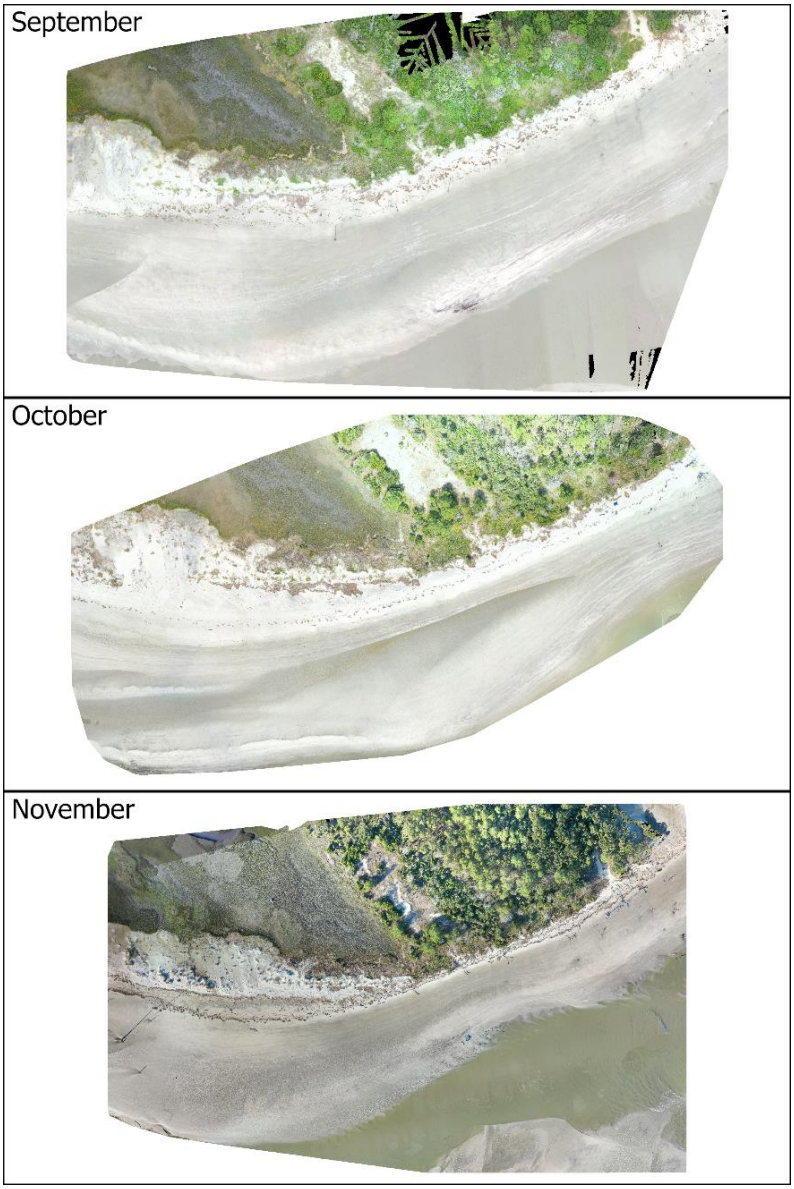

Figure 9: Orthophotos generated from all three survey campaigns using UAV imagery. Note the channel which separated the beach from the sand bar that forms part of the ebb tidal delta.

Figure 10: Mild scarping at the foredune foot during the November survey.

3.5 Long Term Beach Change

DoDs comparing the November UAV survey to lidar-derived DEMs appear similar to the DoD comparing November to October DSMs, with notable erosion in the central portion, but accretion in other areas. At the southernmost portion of the DoD, the high levels of accretion and rippled surface indicate that this area was once a part of a channel where tidal currents flow through the ebb tidal delta, as seen in the November orthophoto in Figure 9. The beach here had grown wider by November 2020, with a shallower slope. This is shown in all DoDs, with significant elevation increase close to the water, but elevation decrease closer to the dunes. While in this portion, the outflow channel has retreated seaward in this portion of the DoD, it has crept slightly landward in the central portion, where the edge of the rippled channel bottom is visible in the November orthophoto and DoDs. At the foredune ridge, there is a significant rise in elevation, although this is most likely due to vegetation on top of the dunes, that was not filtered out of the drone DSM. Little to no retreat of the foredune is evident.

Analysis of the foredune position in older lidar data compared to the 2020 UAV flight shows a persistent trend of shoreline retreat. In the primary area of interest covered by both UAV and pole photogrammetry surveys, from 1997 to 2006, the foredune retreated landward by roughly 0-65 m, by 0-44 m between 2006 and 2010, and 23-90 m from 2010 to 2020. Over time, the

foredune shifted from showing a clear corner at the inlet mouth in the earlier surveys to a more gradual curve, as seen in Figure 12.

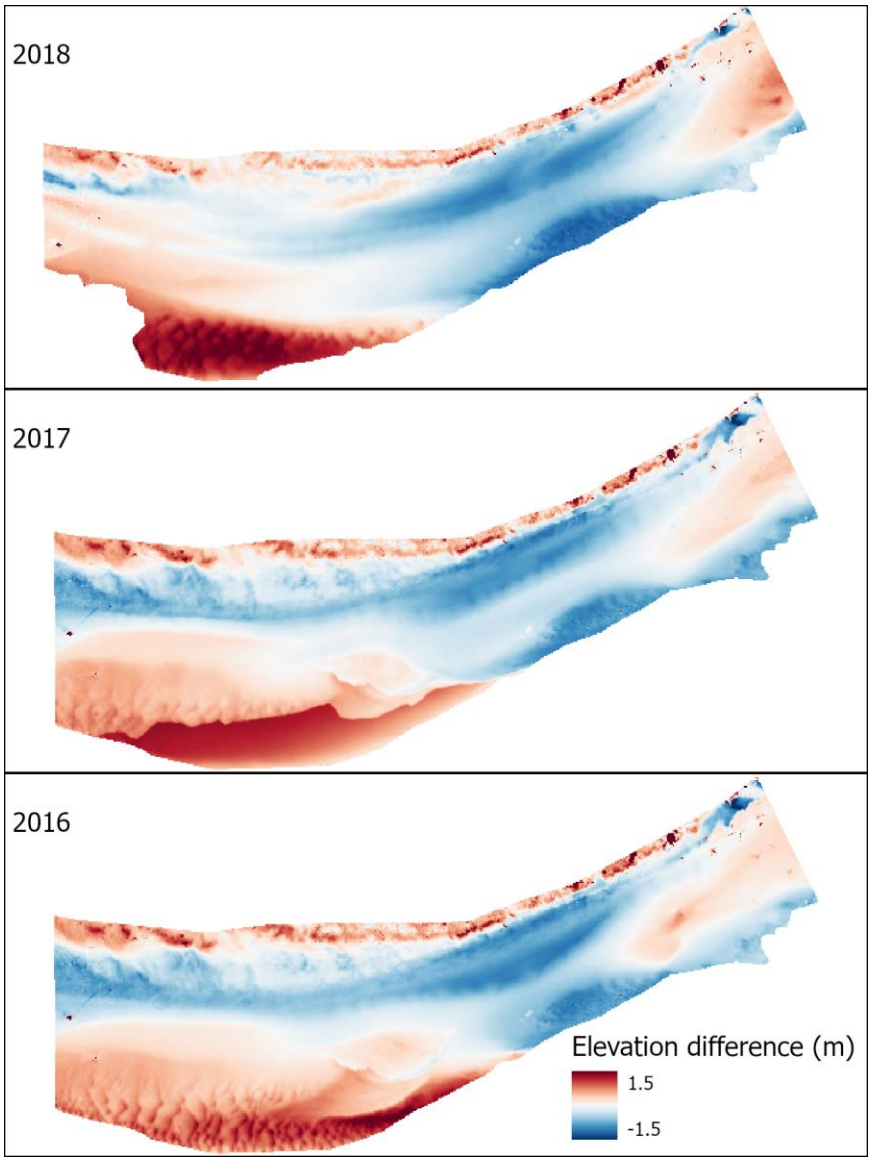

Figure 11: DEMs of Difference comparing the November UAV survey to lidar-derived DEMs from 2016, 2017, and 2018.

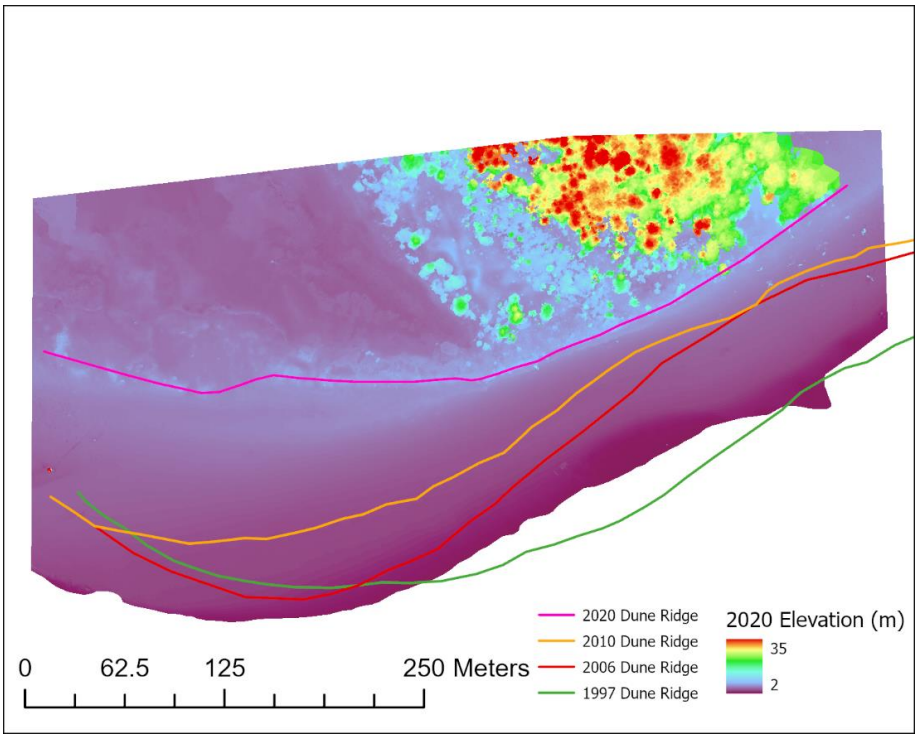

Figure 12: Dune ridge migration from 1997-2020. Dune ridge lines were mapped using lidar surveys from 1997, 2006, and 2010, and the November 2020 UAV survey.

4. Discussion

Results show that pole photogrammetry, while initially very inexpensive to purchase equipment, becomes much more expensive due to the slow rate of image acquisition and long processing times. The time cost of conducting a pole photogrammetry survey may be negligible for small study areas, but rapidly increases as study area increases. Mounting the pole and camera on a vehicle or autonomous rover (or Unmanned Ground Vehicle / UGV) capable of moving at higher speed and automatically following a preplanned route, may be able to drastically reduce the time required to acquire imagery. This may also improve the quality of the pole photogrammetry products, as an automated rover would be able to follow perfectly straight lines and maintain constant spacing between transects, which is difficult to do on foot on an open beach with no visual landmarks.

The quality of UAV-derived DSMs and orthophotos is much higher than those generated from pole imagery. With high quality products and ease of executing surveys, UAV photogrammetry is an excellent tool for routine beach surveying, as shown by Scarelli et al. (2017) and Turner at

al. (2016). Due to the fairly short battery life and thus flight time, UAVs are best suited to smaller study areas, similar in size to the 2 ha area in this study that can be surveyed in a single flight. Alternatively, several successive flights could be strung together to cover a larger area. Due to the long, narrow nature of a beach, fixed-wing drones can be very useful, as used by Long et al. (2016). Fixed wing drones cannot turn as well as multi-rotor systems but can fly longer distances and are thus advantageous where surveys can be completed in a few long, straight transects. With ground control points, no doming was present in any flight but the September survey, which may be caused by the higher flight speed used in this survey or a GCP correction issue. Meanwhile, the pole photogrammetry products were riddled with processing artifacts, making them impossible to incorporate into any meaningful analysis of elevation change. Some of these artifacts, such as the appearance of the operator in orthophotos, are rectifiable by applying a mask to remove the portion of images in which any part of the pole photogrammetry system appears. The inclusion of the pole and operator also causes much of the noise in point clouds, although this is can be removed with cleaning tools in CloudCompare. While the pole photogrammetry system can generate products with extremely high resolution, the sub-5 cm resolution DSMs generated from UAV imagery are more than sufficient. Even lidar surveys of around 1 m resolution are sufficient to discern most beach features. In addition, no increase in resolution is useful without accurate elevation data.

The artifacts and general poor reconstruction affecting the pole photogrammetry products may be the result of several factors. Firstly, a beach environment may simply not be well suited to conducting such close-range photogrammetry surveys. The bare sand of the beach surface can be very plain and featureless, which may be a hinderance to the SfM process. It is noted that the pole photogrammetry performed best near the dunes, where the presence of higher topographic relief and features such as driftwood and reeds lead to better reconstruction. This is clearly seen in Figures 1 and 7, where artifacts do not appear near the dunes. James et al. (2020) show that doming is more common in areas of low topographic relief, and these results show that ghosting is also more common in flat, featureless areas. Other studies incorporating pole photogrammetry have much smaller study areas, with more relief and significant features (e.g., Gonçalves et al., 2016; Wang and Watanabe, 2019; Weßling et al., 2013). In the examples of Wang and Watanabe (2019) and Weßling et al. (2013), the study areas are small archeological sites, where it is easy to aquire a diverse range of look angles and perspectives, whereas on the beach this would be

prohibitively time consuming. In these smaller study areas, the extremely high resolution of pole photogrammetry is an additional advantage, while it is not needed to monitor beach morphology. These results indicate that pole photogrammetry is not very well suited for beach monitoring without major improvements to the image acquisition process or equipment used.

The second factor may be poor geolocation information. The GPS coordinates each GoPro image is tagged with have poor accuracy and precision, especially in the vertical direction, which makes the finding of keypoints difficult. Pairing the GoPro with a small RTK-GNSS unit may be able to improve geolocation information. In addition to accurate geolocation, maintaining a precise camera angle may help as well. Using a gimbal, the drone codes each image with the camera roll, pitch, and yaw, which can assist Pix4D with camera calibration.

A third factor may be insufficient image side overlap, leading to the seams evident in Figure 7. While sidelap is sufficient near the dunes, it is evidently insufficient in the flatter and more featureless parts of the beach. Part of this issue is that it is difficult to maintain perfectly parallel transects on foot, leading to wavering transects and inconsistent overlap. This is another area where an automated system can assist by eliminating human error in route planning and execution. A negative consequence of increasing sidelap is decreased space between transects, thus increasing the total number of transects and time require to complete image acquisition.

Publicly available lidar data are convenient, and still very useful at 1-3 m resolution, but are lacking in temporal resolution. This issue is also noted by Le Mauff et al. (2018), who propose UAVs as a solution when higher temporal resolution is needed. Due to the frequent changes in elevation, and potentially rapid erosion during a large storm, lidar surveys conducted only every few years do not offer much insight into the short time scale processes of a dynamic coastal environment such as this. If lidar surveys were flown monthly, these datasets would be just as, if not more useful than UAV photogrammetry, as large areas can be covered very quickly using a fixed-wing aircraft. However, lidar is very expensive and government resources are often stretched thin. One major benefit of lidar is topobathy, which allows surveying of underwater areas that are impossible for photogrammetry to reconstruct. This would allow surveys to be conducted at any tidal level and observe submerged sandbars and other features important to coastal sediment processes.

Over this three-month study, it is clear that significant changes in the beach do occur on this time scale, although a longer time period is necessary to identify and systematic seasonal or annual trends. Satellite photography and historic lidar imagery show that this beach has experienced a persistent erosion trend since at least 1997, surveys from these three months show more local changes in a particular part of the beach, with erosion in some areas and accretion in others. The changes in elevation observed here are likely the result of larger, more complex processes relating to the ebb tidal delta, in particular the location of the channel that runs along the edge of the study area in Figure 2. These processes are crucial for coastal managers of the inhabited islands directly to the south (Dewees Island, Isle of Palms, and Sullivan's Island), as the dominant flow of sediment on this section of the coast is North to South, and the amount of sediment transferred from island to island across the inlets defines their sediment budgets (Fitzgerald, 1984). The sand bars that form the ebb tide delta are constantly shifting, and occasionally welding to or separating from the beach as sediment makes its way across the inlet. Price inlet, at the north end of Capers Island, functions similarly to Capers Inlet and is well documented by Fitzgerald (1984).

5. Conclusion

UAVs perform excellently for beach surveying and monitoring topographic changes, as corroborated by numerous previous studies (e.g., Brunier et al., 2016; Gonçalves and Henriques, 2015; Mancini et al., 2013; Papakonstantinou et al., 2016; Pérez-Alberti and Trenhaile, 2015; Scarelli et al., 2017; Turner et al., 2016). Owing to the ease of use and speed of image acquisition, UAVs are excellent for routine monitoring of coastal areas, with some limitations. First, study area size is limited by battery life and flight range but can be maximized by flying high altitude and keeping multiple fully charged batteries to execute multiple flights. Two other major limitations are government regulation on UAV flight and poor weather, both of which could totally inhibit flight. Compared to lidar, UAVs offer much cheaper surveys of higher resolution, but covering smaller areas. Therefore, UAVs are best suited to situations where high temporal and/or spatial resolution is needed over a smaller study area.

In both performance and feasibility, UAV photogrammetry is clearly superior to pole photogrammetry. While pole photogrammetry can offer a solution to weather and government

restrictions, the system used here produces very poor DSMs and orthophotos. Despite using the same photogrammetric software, products contained numerous artifacts and were not useable to quantify topographic change. In addition, the slow speed of image acquisition prohibits the implementation of pole photogrammetry in large study areas and can make surveys extremely costly due to long processing and image acquisition times. While UAVs have become a mature platform for Structure from Motion surveys, pole photogrammetry is not as well explored, and requires significant development to be successfully employed in beach environment.

6. References

Boruff, B.J., Emrich, C., Cutter, S.L., 2005. Erosion Hazard Vulnerability of US Coastal Counties. J. Coast. Res. 215, 932–942. https://doi.org/10.2112/04-0172.1

Brasington, J., Langham, J., Rumsby, B., 2003. Methodological sensitivity of morphometric estimates of coarse fluvial sediment transport. Geomorphology 53, 299–316. https://doi.org/10.1016/S0169-555X(02)00320-3

Brodie, K.L., Bruder, B.L., Slocum, R.K., Spore, N.J., 2019. Simultaneous Mapping of Coastal Topography and Bathymetry from a Lightweight Multicamera UAS. IEEE Trans. Geosci. Remote Sens. 57, 6844–6864. https://doi.org/10.1109/TGRS.2019.2909026

Brunier, G., Fleury, J., Anthony, E.J., Gardel, A., Dussouillez, P., 2016. Close-range airborne Structure-from-Motion Photogrammetry for high-resolution beach morphometric surveys: Examples from an embayed rotating beach. Geomorphology 261, 76–88. https://doi.org/10.1016/j.geomorph.2016.02.025

Casella, E., Rovere, A., Pedroncini, A., Mucerino, L., Casella, M., Cusati, L.A., Vacchi, M., Ferrari, M., Firpo, M., 2014. Study of wave runup using numerical models and low-altitude aerial photogrammetry: A tool for coastal management. Estuar. Coast. Shelf Sci. 149, 160–167. https://doi.org/10.1016/j.ecss.2014.08.012

Castillo, C., Pérez, R., James, M.R., Quinton, J.N., Taguas, E. V., Gómez, J.A., 2012. Comparing the Accuracy of Several Field Methods for Measuring Gully Erosion. Soil Sci. Soc. Am. J. 76, 1319–1332. https://doi.org/10.2136/sssaj2011.0390

Dietrich, J.T., 2017. Bathymetric Structure-from-Motion: extracting shallow stream bathymetry from multi-view stereo photogrammetry. Earth Surf. Process. Landforms 42, 355–364. https://doi.org/10.1002/esp.4060

Eltner, A., Kaiser, A., Castillo, C., Rock, G., Neugirg, F., Abellán, A., 2016. Image-based surface reconstruction in geomorphometry-merits, limits and developments. Earth Surf. Dyn. 4, 359–389. https://doi.org/10.5194/esurf-4-359-2016

Fitzgerald, D.M., 1984. Interactions between the ebb-tidal delta and landward shoreline: Price Inlet, South Carolina. J. Sediment. Petrol. 54, 1303–1318. https://doi.org/10.1306/212F85C6-2B24-11D7-8648000102C1865D

Fonstad, M.A., Dietrich, J.T., Courville, B.C., Jensen, J.L., Carbonneau, P.E., 2013. Topographic structure from motion: A new development in photogrammetric measurement. Earth Surf. Process. Landforms 38, 421–430. https://doi.org/10.1002/esp.3366

Galgano, F., 2007. Types and causes of beach erosion anomaly areas in the U.S east coast barrier island system: stabilized tidal inlets. Middle states Geogr. 40, 158–170.

Gesch, D.B., 2018. Best practices for elevation-based assessments of sea-level rise and coastal

flooding exposure. Front. Earth Sci. 6. https://doi.org/10.3389/feart.2018.00230

Giambastiani, B.M.S., Antonellini, M., Oude Essink, G.H.P., Stuurman, R.J., 2007. Saltwater intrusion in the unconfined coastal aquifer of Ravenna (Italy): A numerical model. J. Hydrol. 340, 91–104. https://doi.org/10.1016/j.jhydrol.2007.04.001

Gonçalves, J.A., Henriques, R., 2015. UAV photogrammetry for topographic monitoring of coastal areas. ISPRS J. Photogramm. Remote Sens. 104, 101–111. https://doi.org/10.1016/j.isprsjprs.2015.02.009

Gonçalves, J.A., Moutinho, O.F., Rodrigues, A.C., 2016. Pole photogrammetry with an action camera for fast and accurate surface mapping. Int. Arch. Photogramm. Remote Sens. Spat. Inf. Sci. - ISPRS Arch. 2016-Janua, 571–575. https://doi.org/10.5194/isprsarchives-XLI-B1-571-2016

Harwin, S., Lucieer, A., 2012. Assessing the accuracy of georeferenced point clouds produced via multi-view stereopsis from Unmanned Aerial Vehicle (UAV) imagery. Remote Sens. 4, 1573–1599. https://doi.org/10.3390/rs4061573

Holman, R., Plant, N., Holland, T., 2013. CBathy: A robust algorithm for estimating nearshore bathymetry. J. Geophys. Res. Ocean. 118, 2595–2609. https://doi.org/10.1002/jgrc.20199

Houser, C., Hapke, C., Hamilton, S., 2008. Controls on coastal dune morphology, shoreline erosion and barrier island response to extreme storms. Geomorphology 100, 223–240. https://doi.org/10.1016/j.geomorph.2007.12.007

Houser, C., Wernette, P., Rentschlar, E., Jones, H., Hammond, B., Trimble, S., 2015. Post-storm beach and dune recovery: Implications for barrier island resilience. Geomorphology 234, 54–63. https://doi.org/10.1016/j.geomorph.2014.12.044

Inman, D.L., Elwany, M.H.S., Jenkins, S.A., 1993. Shorerise and bar-berm profiles on ocean beaches. J. Geophys. Res. 98. https://doi.org/10.1029/93jc00996

James, L.A., Hodgson, M.E., Ghoshal, S., Latiolais, M.M., 2012. Geomorphic change detection using historic maps and DEM differencing: The temporal dimension of geospatial analysis. Geomorphology 137, 181–198. https://doi.org/10.1016/j.geomorph.2010.10.039

James, M.R., Antoniazza, G., Robson, S., Lane, S.N., 2020. Mitigating systematic error in topographic models for geomorphic change detection: accuracy, precision and considerations beyond off-nadir imagery. Earth Surf. Process. Landforms 45, 2251–2271. https://doi.org/10.1002/esp.4878

James, M.R., Robson, S., 2014. Mitigating systematic error in topographic models derived from UAV and ground-based image networks. Earth Surf. Process. Landforms 39, 1413–1420. https://doi.org/10.1002/esp.3609

James, M.R., Robson, S., 2012. Straightforward reconstruction of 3D surfaces and topography with a camera: Accuracy and geoscience application. J. Geophys. Res. Earth Surf. 117, 1–17. https://doi.org/10.1029/2011JF002289

Kasvi, E., Salmela, J., Lotsari, E., Kumpula, T., Lane, S.N., 2019. Comparison of remote sensing based approaches for mapping bathymetry of shallow, clear water rivers. Geomorphology 333, 180–197. https://doi.org/10.1016/j.geomorph.2019.02.017

Kim, H., Lee, S.B., Min, K.S., 2017. Shoreline Change Analysis using Airborne LiDAR Bathymetry for Coastal Monitoring. J. Coast. Res. 79, 269–273. https://doi.org/10.2112/si79-055.1

Kulp, S., Strauss, B.H., 2016. Global DEM errors underpredict coastal vulnerability to sea level rise and flooding. Front. Earth Sci. 4, 1–8. https://doi.org/10.3389/feart.2016.00036

Kulp, S.A., Strauss, B.H., 2018. CoastalDEM: A global coastal digital elevation model improved from SRTM using a neural network. Remote Sens. Environ. 206, 231–239. https://doi.org/10.1016/j.rse.2017.12.026

Landry, C.E., Keeler, A.G., Kriesel, W., 2003. An Economic Evaluation of Beach Erosion Management Alternatives. Mar. Resour. Econ. 18, 105–127.

Le Mauff, B., Juigner, M., Ba, A., Robin, M., Launeau, P., Fattal, P., 2018. Coastal monitoring solutions of the geomorphological response of beach-dune systems using multi-temporal LiDAR datasets (Vendée coast, France). Geomorphology 304, 121–140. https://doi.org/10.1016/j.geomorph.2017.12.037

Leatherman, S.P., Zhang, K., Douglas, B.C., 2000. Sea level rise shown to drive coastal erosion. Eos (Washington. DC). 81, 55–57. https://doi.org/10.1029/00EO00034

Long, N., Millescamps, B., Pouget, F., Dumon, A., Lachaussée, N., Bertin, X., 2016. Accuracy assessment of coastal topography derived from uav images. Int. Arch. Photogramm. Remote Sens. Spat. Inf. Sci. - ISPRS Arch. 2016-Janua, 1127–1134. https://doi.org/10.5194/isprsarchives-XLI-B1-1127-2016

Mancini, F., Dubbini, M., Gattelli, M., Stecchi, F., Fabbri, S., Gabbianelli, G., 2013. Using unmanned aerial vehicles (UAV) for high-resolution reconstruction of topography: The structure from motion approach on coastal environments. Remote Sens. 5, 6880–6898. https://doi.org/10.3390/rs5126880

Masselink, G., Pattiaratchi, C.B., 2001. Seasonal changes in beach morphology along the sheltered coastline of Perth, Western Australia. Mar. Geol. 172, 243–263. https://doi.org/10.1016/S0025-3227(00)00128-6

Morton, R.A., Sallenger, A.H., 2003. Morphological impacts of extreme storms on sandy beaches and barriers. J. Coast. Res. 19, 560–573.

Mulhern, J.S., Johnson, C.L., Martin, J.M., 2017. Is barrier island morphology a function of tidal and wave regime? Mar. Geol. 387, 74–84. https://doi.org/10.1016/j.margeo.2017.02.016

Papakonstantinou, A., Topouzelis, K., Pavlogeorgatos, G., 2016. Coastline zones identification and 3D coastal mapping using UAV spatial data. ISPRS Int. J. Geo-Information 5, 1–14. https://doi.org/10.3390/ijgi5060075

Pérez-Alberti, A., Trenhaile, A.S., 2015. An initial evaluation of drone-based monitoring of boulder beaches in Galicia, north-western Spain. Earth Surf. Process. Landforms 40, 105–111. https://doi.org/10.1002/esp.3654

Pikelj, K., Ružić, I., Ilić, S., James, M.R., Kordić, B., 2018. Implementing an efficient beach erosion monitoring system for coastal management in Croatia. Ocean Coast. Manag. 156, 223–238. https://doi.org/10.1016/j.ocecoaman.2017.11.019

Quartel, S., Kroon, A., Ruessink, B.G., 2008. Seasonal accretion and erosion patterns of a microtidal sandy beach. Mar. Geol. 250, 19–33. https://doi.org/10.1016/j.margeo.2007.11.003

Rossi, R.K., 2017. Evaluation of `Structure-from-Motion' from a Pole-Mounted Camera for Monitoring Geomorphic Change. All Grad. Theses Diss.

Scarelli, F.M., Sistilli, F., Fabbri, S., Cantelli, L., Barboza, E.G., Gabbianelli, G., 2017. Seasonal dune and beach monitoring using photogrammetry from UAV surveys to apply in the ICZM on the Ravenna coast (Emilia-Romagna, Italy). Remote Sens. Appl. Soc. Environ. 7, 27–39. https://doi.org/10.1016/j.rsase.2017.06.003

Sexton, W.J., Hayes, M.O., 1991. The geologic impact of Hurricane Hugo and post-storm shoreline recovery along the undeveloped coastline of South Carolina, Dewees Island to the Santee Delta. J. Coast. Res. Spec. Issue 8, 275–290.

Slocum, R.K., Wright, W., Parrish, C., Costa, B., Sharr, M., Battista, T.A., 2019. Guidelines for Bathymetric Mapping and Orthoimage Generation using sUAS and SfM, An Approach for Conducting Nearshore Coastal Mapping. NOAA Technical Memorandum NOS NCCOS 265 83. https://doi.org/10.25923/07mx-1f93

Smith, M.D., Slott, J.M., McNamara, D., Brad Murray, A., 2009. Beach nourishment as a dynamic capital accumulation problem. J. Environ. Econ. Manage. 58, 58–71. https://doi.org/10.1016/j.jeem.2008.07.011

Snavely, N., Seitz, S.M., Szeliski, R., 2008. Modeling the world from Internet photo collections. Int. J. Comput. Vis. 80, 189–210. https://doi.org/10.1007/s11263-007-0107-3

Stockdon, H.F., Doran, K.J., Thompson, D.M., Sopkin, K.L., Plant, N.G., Sallenger, A.H., 2012. National Assessment of Hurricane-Induced Coastal Erosion Hazards : Gulf of Mexico. U.S.

Geol. Surv. Open-File Rep. 2012-1084 51 p.

Taddia, Y., Stecchi, F., Pellegrinelli, A., 2020. Coastal mapping using dji phantom 4 RTK in post-processing kinematic mode. Drones 4, 1–19. https://doi.org/10.3390/drones4020009

Taylor, E.B., Gibeaut, J.C., Yoskowitz, D.W., Starek, M.J., 2015. Assessment and monetary valuation of the storm protection function of beaches and foredunes on the Texas coast. J. Coast. Res. 31, 1205–1216. https://doi.org/10.2112/JCOASTRES-D-14-00133.1

The Heinz Center, 2000. Evaluation of Coastal Hazards. Washington, DC.

Turner, I.L., Harley, M.D., Drummond, C.D., 2016. UAVs for coastal surveying. Coast. Eng. 114, 19–24. https://doi.org/10.1016/j.coastaleng.2016.03.011

Ullman, S., 1979. The interpretation of structure from motion. Proc. R. Soc. Lond. B. Biol. Sci. 203, 405–426. https://doi.org/10.1098/rspb.1979.0006

Vaaja, M., Hyyppä, J., Kukko, A., Kaartinen, H., Hyyppä, H., Alho, P., 2011. Mapping topography changes and elevation accuracies using a mobile laser scanner. Remote Sens. 3, 587–600. https://doi.org/10.3390/rs3030587

Wang, T., Watanabe, T., 2019. Impact of recreational activities on an unmanaged alpine campsite: The case of Kuro-dake Campsite, Daisetsuzan National Park, Japan. Environ. - MDPI 6. https://doi.org/10.3390/environments6030034

Weßling, R., Maurer, J., Krenn-leeb, A., 2013. Structure from Motion for Systematic Single Surface Documentation of Archaeological Excavations 40.

Westoby, M.J., Brasington, J., Glasser, N.F., Hambrey, M.J., Reynolds, J.M., 2012. "Structure-from-Motion" photogrammetry: A low-cost, effective tool for geoscience applications. Geomorphology 179, 300–314. https://doi.org/10.1016/j.geomorph.2012.08.021

Zhang, K., Douglas, B.C., Leatherman, S.P., 2004. Global Warming and Coastal Erosion. Clim. Change 64, 41–58. https://doi.org/10.1023/B:CLIM.0000024690.32682.48